Elastohydrodynamic lubrication and wear modelling of the knee joint replacements with surface topography

Goa, Leiming; Hua, Zikai; Hewson, Robert; Andersen, Michael Skipper; Jin, Zhongmin

Published in:
Biosurface and Biotribology

DOI (link to publication from Publisher):
10.1049/bsbt.2017.0003

Publication date:
2018

Document Version
Publisher's PDF, also known as Version of record

Biosurface and Biotribology

Research Article

Elastohydrodynamic lubrication and wear modelling of the knee joint replacements with surface topography

ISSN 2405-4518
Received on 21st November 2017
Revised on 23rd January 2018
Accepted on 1st February 2018
doi: 10.1049/bsbt.2017.0003
www.ietdl.org

Leiming Gao[1] ✉, Zikai Hua[2], Robert Hewson[1], Michael Skipper Andersen[3], Zhongmin Jin[4,5]

[1]*Department of Aeronautics, Imperial College London, London, UK*
[2]*School of Mechatronics Engineering and Automation, Shanghai University, Shanghai, People's Republic of China*
[3]*Department of Materials and Production, Aalborg University, 9100 Aalborg, Denmark*
[4]*Southwest Jiaotong University, Chengdu, People's Republic of China*
[5]*Tribology Research Institute, School of Mechanical Engineering, University of Leeds, Leeds, UK*
✉ *E-mail: leiming.gao@gmail.com*

Abstract: This numerical study predicted wear of lubricated total knee replacements with the existing of textured surface and the possibility of surface designs to reduce wear. In the first part, a wear model of metal-on-polyethylene total knee replacement was developed. The medial and lateral knee compartments was accounted for separately, with the contact force and motion during walking cycles applied. An adapted Archard wear formula was employed where the wear factor was an exponential function of the 'Lambda ratio' (film thickness to the average roughness). Wear of the soft bearing surface (polyethylene insert) was simulated with regularly geometry update until a steady-state wear observed. In the second part, the effect of surface topography of the knee replacements was investigated. The surface texturing techniques have shown promising benefit to machine components in many areas of engineering practice. The texture parameters were designed using the Taguchi method for the geometry, size, and distribution of the micro dimples. It was observed that the lateral compartment may benefit from surface texturing if dimples were properly designed, while the texturing showed hardly advantageous effect on the medial surface in terms of lubrication enhancement and wear reduction. Some results were presented in the 6th World Tribology Conference.

1 Introduction

The knee joint replacement is a surgical treatment for damaged knee joints to retrieve their functions and relief the pain. There were 108,713 knee replacement procedures in the UK in 2016 and this number has been increased by 3.8% from last year, among those ~6% of the implants were revision procedures [1, 2]. The probability revision after 10-years-survivial is around 5% in an average age, while for patients younger than 55 years old the rate could reach 15–20% [2]. Polyethylene is still the predominant material for the tibial insert or the entire tibial component. Aseptic loosening, pain and infection are almost the top three reasons to the failure of the knee implants, in which aseptic loosening is regarded to be a result of the adverse reactions between the polyethylene wear debris and peri-implant bone and tissues. It is therefore important to investigate the wear mechanism in order to reduce wear and improve the survival time of the implants.

To evaluate the wear performance of a knee implant before the clinic, wear test is normally carried out in physical joint simulators. However, it is both time and economic costing and the tests are limited to the complicated designs requested for joint simulators to simulate various motions in human activities. For example, it generally takes five to six months to simulate a five-years-service of a hip or knee implants. With the fast development of computing techniques, the design prototype of many products in commercial and industrial have been changed and numerical simulations have been used as an important tool in both design and testing stage of those products. Similarly, for joint replacements, numerical modelling may play an important role in the design and performance predicting of new and more reliable joint replacements.

Computational models based on finite element analysis (FEA) have been widely developed in both joint scale and the musculo-skeletal body scale to analyse the contact stress and stability of the knee implants subjected to complex dynamic activities [3]. There are a number of FEA studies on the wear modelling of knee bearing surfaces [4–8], however, lubrication was not explicitly addressed in most of those wear models, mainly because of the complicated wear mechanism when lubrication is involved, and particularly for the multiple contacts and complicated geometry in the knee joints than hips.

There are just a few numerical studies on the lubrication of artificial knee joints. An early lubrication model of knee implants was developed by Tandon and Jaggi in 1979 [9], with two regions described, the fluid flowing between narrow gap of the joint surfaces and flowing into one porous surface material. Jin *et al.* [10] developed an elastohydrodynamic lubrication (EHL) model with simplified ellipsoidal geometry to represent the knee contact and coupled with the general central film thickness formula through an ellipticity coefficient. In their work, the contact area and lubricant film thickness were predicted with various geometrical parameters under walking conditions. Recently, the authors have developed an advanced wear model for lubricated hip joints in which lubrication parameters were coupled in the wear factor through an adapted Archard wear formula [11]. This wear model has applied to knee replacements in this study. The effect of surface texturing on the lubrication and wear of knee replacements was also investigated.

2 Methodology

2.1 Materials and geometry

A total knee replacement (TKR), made of ultra-high-molecular-weight polyethylene (UHMWPE) tibial insert and metallic (or ceramic) femoral component, was investigated. The contacts between the femoral condyles and tibial insert in the medial and lateral compartments were both represented by the ball-and-socket geometry [10, 12] with uniform curvature radii, as shown in Fig. 1. The tibial surface was simplified as a saucer with the polar

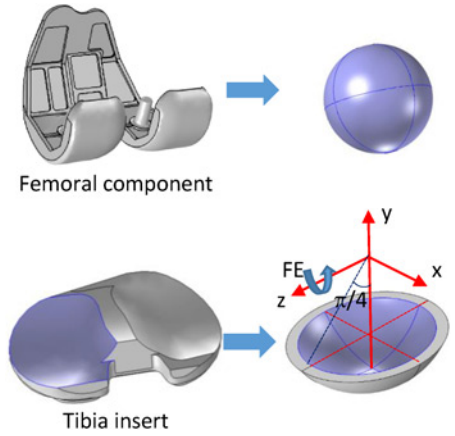

Fig. 1 *Simplification of knee geometry in the wear model*

Table 1 Material and geometrical parameters

radius of both femoral condyles	50 mm
radial clearance	0.5 mm
tibia socket thickness	7 mm
elastic modulus of polyethylene	1 GPa
Poisson's ratio of polyethylene	0.4
RMS roughness (R_a) of tibia polyethylene surface	0.5 μm

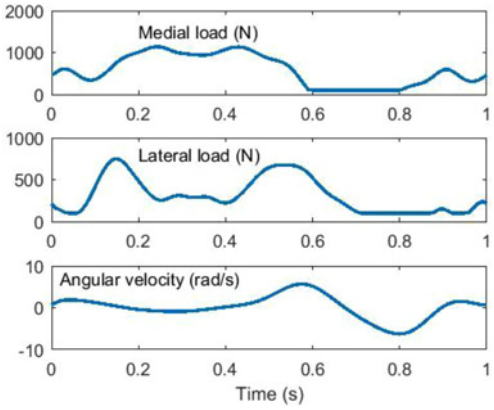

Fig. 2 *Medial and lateral load and the angular velocity of knee joint in gait cycles*

angle from the y-axis of $\pi/4$. The femoral condyles that were made of hard materials were assumed to be rigid due to significantly larger modulus than the counter surface, thus only the soft tibial insert deformed. The elastic modulus for polyethylene varied in a large range of 0.5–8 GPa [13], and a value of 1 GPa was chosen to represent the UHMWPE insert [14, 15]. The geometrical parameters and mechanical properties of the materials are chosen based on reports of knee replacements in the literature and listed in Table 1 [16, 17].

In the numerical model, the femoral condyles were rotating against the stationary tibial insert in flexion–extension direction. The load applied on the knee bearing surface was measured from in vivo measurements of ground contact force in walking in medial and lateral compartment separately [18], and the angular speed of flexion–extension rotation was predicted using the model developed by Marra *et al.* [19], as shown in Fig. 2.

2.2 Mixed lubrication modelling

A mixed EHL model was adopted to obtain the fluid pressure and film thickness field, which were coupled into the wear model. In the full film regime, the thin film lubrication addressing the non-Newtonian shear-thinning properties of the human joint synovial fluid was governed by the Reynolds equation formulated in spherical coordinates (θ, ϕ) [20]

$$\frac{\partial}{\partial\varphi}\left(\frac{h^3}{\eta}\frac{\partial p}{\partial\varphi}\right)+\sin\theta\frac{\partial}{\partial\theta}\left(\frac{h^3}{\eta}\sin\theta\frac{\partial p}{\partial\theta}\right)=-6R^2\sin^2\theta\left(\omega\frac{\partial h}{\partial\varphi}+2\frac{\partial h}{\partial t}\right) \tag{1}$$

where p is the fluid pressure, h is the fluid film thickness, η is the viscosity of the joint synovial fluid, R is the uniform curvature radius of the tibial insert, and ω is the flexion–extension angular rotation speed (around the z-axis in Fig. 1). The boundary conditions of pressure were applied by setting the pressure to zero immediately if a negative pressure was obtained during iteration, at the inlet and outlet boundaries of the calculation domain. The film thickness (i.e. geometry of gap between the two bearing surfaces) was composed of the rigid geometric gap, eccentricities due to load and surface deformation

$$h(\varphi,\theta)=c-e_x\sin\theta\cos\varphi-e_y\sin\theta\sin\varphi-e_z\cos\theta+\delta(p) \tag{2}$$

In which c is the radial clearance of the femoral component and tibial insert, e_x, e_y, e_z are the eccentricity components. The elastic deformation (δ) of the polyethylene tibial surface was described by the spring model, which was proportional to the local pressure through a set coefficient [21].

In the boundary lubrication regime, it was assumed that a thin molecular layer of synovial fluid always absorbed on the surface, with a thickness of $h_B = 20$ nm, i.e. the boundary film thickness when there was no hydrodynamic flow. When the calculated value of h was smaller than h_B, film thickness equation was switched to the boundary lubrication mode, i.e. $h(p)=h_B$, and the asperity contact pressure at that local point corrected to replace the fluid pressure derived from the Reynolds equation [11].

The shear-thinning viscosity characteristic of synovial fluid was described by [22]

$$\eta=\eta_\infty+\frac{\eta_0-\eta_\infty}{1+\alpha(\dot\gamma)^\beta} \tag{3}$$

Based on experimental tests of various synovial fluids, the limit viscosity at the theoretical zero (η_0) and infinite shear rate (η_∞) was 40 and 0.005 Pa·s, and the values for parameters α and β were set to 9.54 and 0.73, respectively. The pressure variation across the film thickness direction was ignored due to the very thin films considered. An average shear rate ($\dot\gamma$) was used and calculated as the ratio of relative surface velocity to film thickness. The external loading components $w_{x,\,y,\,z}$ were balanced by the pressure integrated into three Cartesian coordinates. It needs to be noted that the centre of the femoral component could move towards all three directions as the contact is described in three-dimensional (3D) curvature radii in this model, rather than the 2D radii in point contact for the simplified ball-on-plane geometry, though only one rotation was considered

$$w_{x,y,z}=R^2\int_\phi\int_\theta p_{x,y,z}\,\mathrm{d}\theta\,\mathrm{d}\phi \tag{4}$$

The multi-grid method was used to solve the equation system and details of numerical procedures are referred to [20].

2.3 Wear modelling

An advanced wear model recently developed by Gao *et al.* [11] was employed, which addressed the mixed lubricated condition rather than only a dry contact, to predict the abrasive wear evolution on the bearing surfaces of joint replacements. The level of wear of TKRs which operate in a mixed lubricated regime was dependent on the film thickness and the bearing surface roughness. Based on

an adapted Archard wear formula [11, 23, 24] the wear factor was proposed as a power function of the 'λ ratio', i.e. the ratio of film thickness to the average surface roughness (R_a). As only 1D rotation was included currently the wear due to the cross-shear motion was not considered in this study. The linear wear rate, i.e. wear depth per unit time, of the implant bearing surfaces caused by abrasion wear was described as

$$\text{wear rate} = \begin{cases} k_w pv\left(\frac{1}{\lambda}\right)^a, & \text{if } \lambda < 3 \\ 0, & \text{if } \lambda \geq 3 \end{cases} \quad (5)$$

$$\lambda = h/R_a \quad (6)$$

where k_w is the constant wear parameter according to experimental tests [13], and the value of 1×10^{-8} mm^3/Nm was chosen here. In this model, the wear coefficient is a function of the lambda ratio ($k_w \lambda^{-a}$), if compared with other models. With the constant value $k_w = 1 \times 10^{-8}$ and the lambda ratio between 0.2 (at the average minimum film thickness of ~0.10 μm) and 3 (threshold at full film regime), the wear coefficient ranged in 0.85×10^{-9}–3.68×10^{-7}, which was compared to the literature [7, 13, 25, 26]. The power term (a) determines how sensitive the transition to wear occurs with a decreasing film thickness, and its value was chosen as 2.24 [11]. For this value, it needs to be noted that experimental tests are required to validate which is a limitation of the model. The average surface roughness of the tibial polyethylene surface was 0.5 μm [27]. The local relative sliding speed of the two surfaces is calculated as

$$v = \sqrt{v_\theta^2 + v_\varphi^2} \quad (7)$$

$$\begin{cases} v_\theta = -R\omega_x \sin\varphi \\ v_\varphi = -R\omega_x \cos\varphi \cos\theta \end{cases} \quad (8)$$

The wear depth at each mesh point (i, j) was summed over all time steps (n) in one cycle

$$W_{L\_cyc}^{i,j} = \sum_{k=1}^{n} W_L^{i,j}(k) \quad (9)$$

Within N gait cycles the wear depth per cycle was approximately the same if the change of surface profile due to wear was not large enough to affect the lubrication. Thus the wear depth per N cycles was calculated as

$$W_{L\_tot}^{i,j} \simeq N \cdot W_{L\_cyc}^{i,j} \quad (10)$$

The wear depth at each point (i, j) during N gait cycles can be approximately evaluated as the number of cycles multiplied with the wear depth per cycle, if the change of surface profile was not large enough to affect the lubrication within N cycles

$$W_{\text{vol}} = \sum_{i=1}^{m}\sum_{j=1}^{m}(W_{L\_tot}^{i,j} \times A_{i,j}) \quad (11)$$

$$A_{i,j} \simeq \left(\pi R/m\right)^2 \cdot \sin\theta_{i,j} \quad (12)$$

A flowchart describing the wear simulation procedure can be found in [11].

2.4 Surface texturing

The surface texturing techniques have shown promising benefit to machine components in many areas of engineering practice particularly in friction reduction and lubrication enhancement [28, 29]. The dimples were distributed only on the tibial component surface and the counter femoral bearing surface was assumed smooth, since the tibial surface was more deformable.

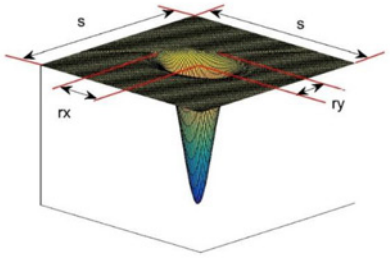

Fig. 3 *Schematic of dimple geometry*

Table 2 Design of experiments on dimple parameters

Run no.	R_x, mm	R_y/R_x	s/max (R_x, R_y)	σ
0*	0.3	0.5	2.5	0.1
1	0.3	0.5	2.5	0.1
2	0.3	1	3	0.2
3	0.3	2	4	0.4
4	0.5	0.5	3	0.4
5	0.5	1	4	0.1
6	0.5	2	2.5	0.2
7	1	0.5	4	0.2
8	1	1	2.5	0.4
9	1	2	3	0.1

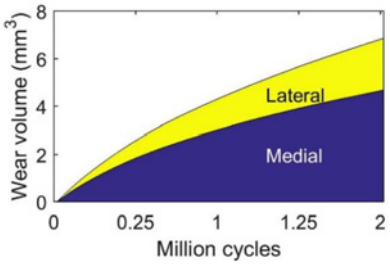

Fig. 4 *Accumulated wear volume variation against time*

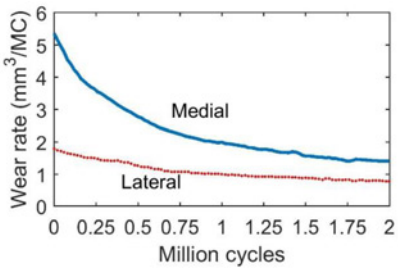

Fig. 5 *Wear rate variation against time*

The geometry of dimples was described by the Gaussian function

$$f(x, y) = \exp\left[-\left(x^2/r_x^2 + y^2/r_y^2\right)/\sigma\right] \quad (13)$$

The experiments of the dimple parameters were designed using the Taguchi orthogonal arrays of totally nine runs with four parameters in three levels. The parameters include r_x, r_y, in (13) and s (the length of each cell square), as shown in Fig. 3. The parameter σ notes the standard deviation in the Gaussian function, and controls the width of the 'bell' shape. The parameters in each run are shown in Table 2. In the run of No. 0, dimples were distributed over all bearing surfaces, while No. 1–9 only on the half entrainment zone, this is because the partially distributed texturing in the inlet zone was reported more potentially benefit to lubrication [30].

Biosurf. Biotribol., 2018, Vol. 4, Iss. 1, pp. 18–23

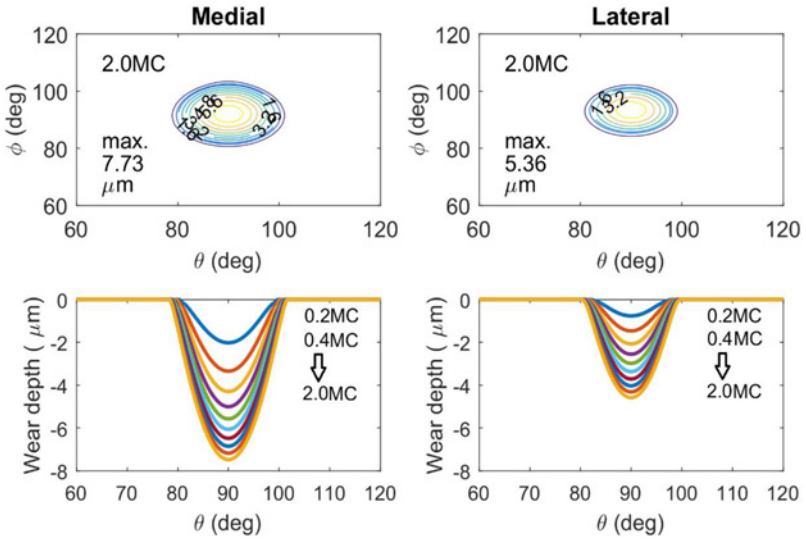

Fig. 6 *Wear scar contours at 2 MC and wear depth evolution at the central cross-section updated by every 0.2 MC*

3 Results

The wear of the knee implant with smooth surfaces was simulated for two million cycles (MC) until reaching a steady-state condition, with a geometry update at each 0.02 MC. The frequency to update the change of surface profile due to wear was tested to make sure that the surface change within the interval of update was not large enough to affect the lubrication solutions. The results of the numerical wear simulations are presented in three aspects.

3.1 Wear in large time scales of MC (no surface texturing)

The accumulated wear volumes were 4.68 and 2.19 mm^3 on the medial and lateral compartments, respectively. The accumulated wear volume simulated in two MC is shown in Fig. 4, where the lateral wear is plotted on top of the medial wear. The wear rates are presented in Fig. 5 and it is clear to observe the wear stage change from the running-in wear (with wear rate of 2–5 mm^3/MC within the first MC) to the steady-state wear (with wear rate of 1.4–2 mm^3/MC in the second MC) in the medial compartment. The wear scar profiles on the polyethylene tibial surface were presented in Fig. 6, which contains the final wear scar contours and the wear depth evolution on the interior-posterior cross-section during the simulated wear process.

3.2 Wear in small time scales of one gait cycle (no surface texturing)

It is interesting to zoom in the time scale from MC to one gait cycle and observe the lubrication parameters and wear generated at each small time instant. Although the amount of wear at such a short time scale is very small, it implied the wear probability distribution over the cyclic time which is clearly relevant to the cyclic loading and motion patterns. The volumetric wear (in percentage) during the first and the last gait cycles of the total wear simulation is presented in Fig. 7. The 'percentage' here means that the wear volume generated at each time instant was divided by the total wear volume in that cycle. The maximum pressure and minimum film thickness in the medial compartment are compared in the first and last wear cycles shown in Fig. 8.

3.3 Wear in one gait cycle with surface texturing

A total number of ten designs of surface texturing were tested using the wear model and the wear reduction (percentage) compared to the non-textured knee implant is presented in Fig. 9. It can be observed

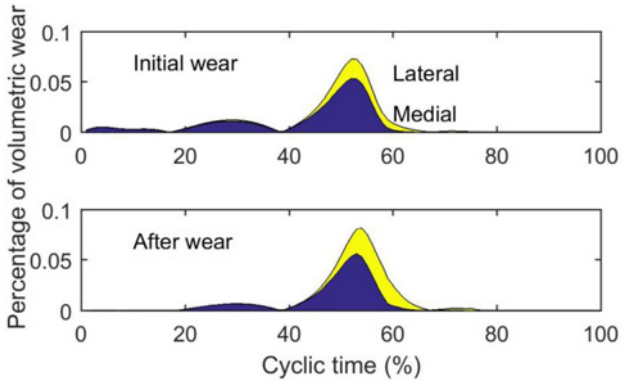

Fig. 7 *Volumetric wear percentage distribution in one walking cycle (lateral wear is plotted on top of medial)*

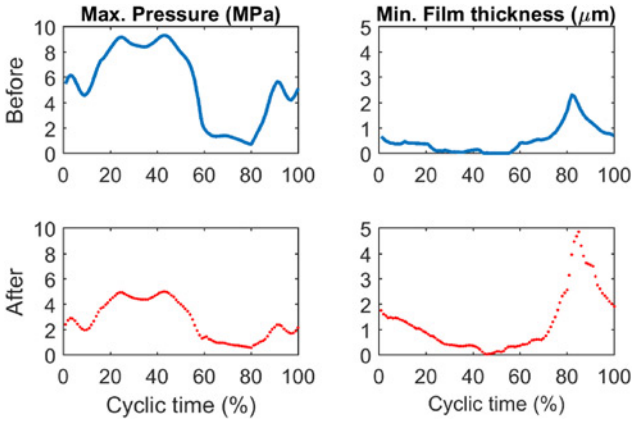

Fig. 8 *Maximum pressure and minimum film thickness compared to the first and last wear cycle (in medial)*

that Nos. 3, 7 and 9 resulted in the lowest wear among all the texture designs. For the lateral compartment, these three experiments reduced wear by ~4%. However, in the medial compartment, no obvious benefit was found and most of the texturing designs even caused slightly more wear. The variations of the minimum film thickness in the non-textured knee joint are compared with the run No. 9 (which is the most beneficial case of the ten runs) shown in Fig. 10.

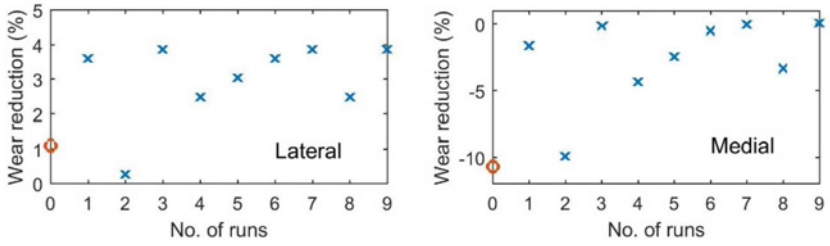

Fig. 9 *Effect of surface texturing parameters on wear reduction (circle notes full domain distribution; crosses note half domain distribution)*

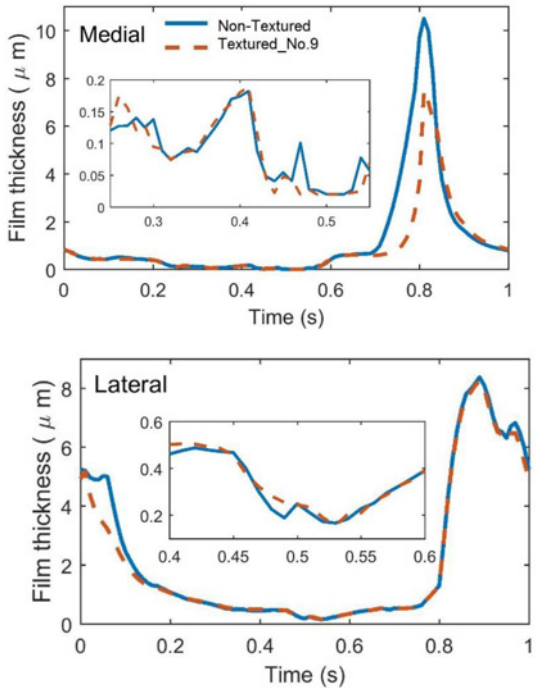

Fig. 10 *Minimum film thickness variations in a gait cycle compared with the non-textured case and No. 9 textured surface case*

4 Discussion

4.1 Lubrication and wear analysis

The surface profile change due to wear leads to a geometrical change in the gap (clearance) between the femoral and tibial bearing surfaces, resulted in the two-stage wear process (severe or abnormal loading conditions are exceptional). The maximum change of the clearance of the knee joint in this study was 7.73 μm in the medial and 5.36 μm in the lateral compartment after 2 MC (the maximum wear depth shown in Fig. 6). This value indicated the effective change to transfer the running-in wear to a steady-state stage. This change causes the two bearing surfaces to have a more similar curvature radius in joint scale (conformity) with a larger lubricated area. Thus, the distribution of pressure became flattened with a lower maximum pressure, subjected to the same loading cycle, and the film thickness is increased, which is clearly observed in Fig. 8. The two-stage non-linear wear trend agrees well with the wear simulator test of hip replacements [31, 32], which has a ball and socket geometry. While linear wear trend was often reported from the knee simulator studies [33, 34], the simplification of the knee geometry is one of the major limitations of the current model resulting in simplified conformity and contact area which are actually more complicated in the knee joints [17, 35].

The real wear process spans in distinct time scales; from chemical reactions between the metal surface and synovial fluid in micro-seconds, to the loading cycle of gait in seconds, and to the lift time of the joints in years (or for joint simulator tests in months). This study simulated the wear process on two time scales, the gait cycle in seconds and millions of gait cycles representing the joint lifetime in years. It is time-efficient to investigate the wear in one gait cycle in order to evaluate what geometrical and loading parameters may reduce wear or cause severe wear. Despite of the wear stage, the highest wear occurred around 55% of the cyclic time, which is just after the second peak loading on medial compartment. It is interesting to note that there were two loading peaks in the gait cycle with similar peak values on both medial and lateral compartments, but the second loading peak (40–60%) generated much more wear than the first one (10–20%). This can be explained in two aspects; the sliding speed was much higher around the second loading peak, which contributes to the higher sliding wear; after the second loading peak the load was released in swing phase, which caused weak squeeze film action to establish the lubricated film, and resulted in a much thinner film as shown in Fig. 10.

4.2 Effect of surface texturing

It has been reported that the micro-textures distributed over the whole contact domain may not provide the best performance compared with that located in the entrainment half zone, instead, it may cause worse lubrication [30]. Thus only one (No. 0) of totally ten runs was designed as 'whole domain surface texturing, and it has been proved with little benefit to the wear reduction. The rest of nine runs (Nos. 1–9) were half textured in the entrainment direction during extension. This is because the major motion of the knee is extension when subjected to most of the load in the standing phase.

In the non-textured knee joint, the thin film (<0.2 μm) occurred at around 50% cyclic time after subjected to the second loading peak when the most wear occurred as discussed in the above section. In the textured joint replacements (take No. 9 for example), a much thicker film (0.2–0.5 μm) was found during 20–60% of cyclic time in the lateral compartment (Fig. 10), thus an increased film thickness and a reduced wear were observed compared to the non-textured joint. However, in the medial compartment that was subjected to larger loads, the film thickness was even decreased compared with the non-textured joint, particularly around 50% cyclic time, thus the total wear was slightly increased. It is difficult to find a direct relationship between any single parameter of texturing and wear, thus conclusion so far can be made is that the surface texture needs to be designed carefully to enhance lubrication and reduce wear for knee joints and further investigation on the specific geometry of knee replacements and loading conditions is required.

Due to the limitations as listed below, the predicted wear may not compared quantitatively to the joint simulator tests.

- The ball and socket geometry with uniform curvature radius instead of a real knee contact geometry. This simplified the conformity and contact area of the knee joints and it a major limitation of the current model.
- Only one load and one motion applied for walking conditions of the knee joints thus cross-shear was not considered.
- The parameters in the wear model need to be determined and validated by experimental tests.

Biosurf. Biotribol., 2018, Vol. 4, Iss. 1, pp. 18–23

5 Conclusions

This paper numerically predicted the sliding wear of metal-on-UHMWP total knee joints, and the possibility of surface texturing designs to reduce wear. A mixed EHL model was coupled in the wear modelling. The medial and lateral knee compartments were accounted for separately, applied with experimentally measured contact force and motion in walking cycles. Wear of the soft bearing surface (polyethylene tibial insert) was simulated with a regular geometry update until a steady-state wear observed. The main conclusions are summarised as

- Lubrication was considered in the wear modelling of the knee joint.
- The lateral contact area may benefit from surface texturing only if dimples were carefully designed, while
- The medial contact area hardly got advantage from surface texturing.

6 Acknowledgment

This work was financially supported by the Imperial Junior Research Fellowship (2015-2018) and Shanghai Natural Science Foundation of China (16ZR1411800). M.S. Andersen was supported by the Sapere Aude program of the Danish Council for Independent Research (DFF-4184-00018).

7 References

[1] 'Summary of Key Facts about Joint Replacement During the 2016 Calendar Year'. 2017. General editor, NHS UK
[2] 'The National Joint Registry's 14th Annual Report'. 2017
[3] Jin, Z.M., Zheng, J., Li, W., *et al.*: 'Tribology of medical devices', *Biosurface Biotribol.*, 2016, **2**, pp. 173–192
[4] Arjmandi, M., Ramezani, M., Giordano, M., *et al.*: 'Finite element modelling of sliding wear in three-dimensional woven textiles', *Tribol. Int.*, 2017, **115**, pp. 452–460
[5] Innocenti, B., Labey, L., Kamali, A., *et al.*: 'Development and validation of a wear model to predict polyethylene wear in a total knee arthroplasty', *Lubricants*, 2014, **2**, pp. 193–205
[6] Netter, J., Hermida, J., Flores-Hernandez, C., *et al.*: 'Prediction of wear in crosslinked polyethylene unicompartmental knee arthroplasty', *Lubricants*, 2015, **3**, pp. 381–393
[7] Abdelgaied, A., Liu, F., Brockett, C., *et al.*: 'Computational wear prediction of artificial knee joints based on a new wear law and formulation', *J. Biomech.*, 2011, **44**, pp. 1108–1116
[8] Zhang, J., Chen, Z.X., Wang, L., *et al.*: 'A patient-specific wear prediction framework for an artificial knee joint with coupled musculoskeletal multibody-dynamics and finite element analysis', *Tribol. Int.*, 2017, **109**, pp. 382–389
[9] Tandon, P.N., Jaggi, S.: 'A model for the lubrication mechanism in knee joint replacements', *Wear*, 1979, **52**, pp. 275–284
[10] Jin, Z.M., Dowson, D., Fisher, J., *et al.*: 'Prediction of transient lubricating film thickness in knee prostheses with compliant layers', *Proc. Inst. Mech. Eng. H-J. Eng. Med.*, 1998, **212**, pp. 157–164
[11] Gao, L., Dowson, D., Hewson, R.W.: 'Predictive wear modelling of the metal-on-metal hip replacements', *J. Biomed. Mater. Res. B, Appl. Biomater.*, 2017, **105**, pp. 497–506
[12] Mongkolwongrojn, M., Wongseedakaew, K., Kennedy, F.E.: 'Transient elastohydrodynamic lubrication in artificial knee joint with non-Newtonian fluids', *Tribol. Int.*, 2010, **43**, pp. 1017–1026
[13] Carr, B.C., Goswami, T.: 'Knee implants – review of models and biomechanics', *Mater. Des.*, 2009, **30**, pp. 398–413
[14] Liau, J.J., Cheng, C.K., Huang, C.H., *et al.*: 'The effect of malalignment on stresses in polyethylene component of total knee prostheses – a finite element analysis', *Clin. Biomech.*, 2002, **17**, pp. 140–146
[15] Jin, Z.M., Dowson, D., Fisher, J.: 'A parametric analysis of the contact stress in ultra-high-molecular-weight polyethylene acetabular cups', *Med. Eng. Phys.*, 1994, **16**, pp. 398–405
[16] Shi, I.F., Wang, C.J., Berryman, F., *et al.*: 'The effect of polyethylene thickness in fixed- and mobile-bearing total knee replacements', *Proc. Inst. Mech. Eng. H-J. Eng. Med.*, 2008, **222**, pp. 657–667
[17] Ardestani, M.M., Moazen, M., Jin, Z.M.: 'Contribution of geometric design parameters to knee implant performance: conflicting impact of conformity on kinematics and contact mechanics', *Knee*, 2015, **22**, pp. 217–224
[18] Fregly, B.J., Besier, T.F., Lloyd, D.G., *et al.*: 'Grand challenge competition to predict in vivo knee loads', *J. Orthopaedic Res.*, 2012, **30**, pp. 503–513
[19] Marra, M.A., Vanheule, V., Fluit, R., *et al.*: 'A subject-specific musculoskeletal modeling framework to predict in vivo mechanics of total knee arthroplasty', *J. Biomech. Eng. Trans. Asme*, 2015, **137**, pp. 020904
[20] Gao, L.M., Wang, F.C., Yang, P.R., *et al.*: 'Effect of 3d physiological loading and motion on elastohydrodynamic lubrication of metal-on-metal total hip replacements', *Med. Eng. Phys.*, 2009, **31**, pp. 720–729
[21] Jalali-Vahid, D., Jagatia, M., Jin, Z.M., *et al.*: 'Prediction of lubricating film thickness in UHMWPE hip joint replacements', *J. Biomech.*, 2001, **34**, pp. 261–266
[22] Gao, L., Dowson, D., Hewson, R.W.: 'A numerical study of non-Newtonian transient elastohydrodynamic lubrication of metal-on-metal hip prostheses', *Tribol. Int.*, 2016, **93**, pp. 486–494
[23] Archard, J.F.: 'Contact and rubbing of flat surfaces', *J. Appl. Phys.*, 1953, **24**, pp. 981–988
[24] Sharif, K.J., Evans, H.P., Snidle, R.W., *et al.*: 'Effect of elastohydrodynamic film thickness on a wear model for worm gears', *Proc. Inst. Mech. Eng. J-J. Eng. Tribol.*, 2006, **220**, pp. 295–306
[25] Fregly, B.J., Sawyer, W.G., Harman, M.K., *et al.*: 'Computational wear prediction of a total knee replacement from in vivo kinematics', *J. Biomech.*, 2005, **38**, pp. 305–314
[26] Goswami, T., Alhassan, S.: 'Wear rate model for UHMWPE in total hip and knee arthroplasty', *Mater. Des.*, 2008, **29**, pp. 289–296
[27] Ruggiero, A., Merola, M., Affatato, S.: 'On the biotribology of total knee replacement: a new roughness measurements protocol on in vivo condyles considering the dynamic loading from musculoskeletal multibody model', *Measurement*, 2017, **112**, pp. 22–28
[28] Gao, L.M., Yang, P.R., Dymond, I., *et al.*: 'Effect of surface texturing on the elastohydrodynamic lubrication analysis of metal-on-metal hip implants', *Tribol. Int.*, 2010, **43**, pp. 1851–1860
[29] Hua, Z.K., Sang, R.Z., Zhang, J.H.: 'Micro and nano-scale surface texturing: an application in ceramic-on-ceramic artificial joint materials', *Nanosci. Nanotechnol. Lett.*, 2012, **4**, pp. 879–882
[30] Gropper, D., Wang, L., Harvey, T.J.: 'Hydrodynamic lubrication of textured surfaces: a review of modeling techniques and key findings', *Tribol. Int.*, 2016, **94**, pp. 509–529
[31] Al-Hajjar, M., Fisher, J., Williams, S., *et al.*: 'Effect of femoral head size on the wear of metal on metal bearings in total hip replacements under adverse edge-loading conditions', *J. Biomed. Mater. Res. B, Appl. Biomater.*, 2013, **101b**, pp. 213–222
[32] Liu, F., Leslie, I., Williams, S., *et al.*: 'Development of computational wear simulation of metal-on-metal hip resurfacing replacements', *J. Biomech.*, 2008, **41**, pp. 686–694
[33] Abdel-Jaber, S., Belvedere, C., Leardini, A., *et al.*: 'Wear simulation of total knee prostheses using load and kinematics waveforms from stair climbing', *J. Biomech.*, 2015, **48**, pp. 3830–3836
[34] Tsukamoto, R., Chen, S., Asano, T., *et al.*: 'Improved wear performance with crosslinked UHMWPE and zirconia implants in knee simulation', *Acta Orthopaedica*, 2006, **77**, pp. 505–511
[35] Zhou, Z.R., Jin, Z.M.: 'Biotribology: recent progresses and future perspectives', *Biosurface Biotribol.*, 2015, **1**, pp. 3–24